SMC-TR-93-64

AEROSPACE REPORT NO.
TR-93(3935)-12

An Ultrasonic Testing Technique for Monitoring the Cure and Mechanical Properties of Polymeric Materials

22 August 1993

Prepared by

E. C. JOHNSON, J. D. POLLCHIK, and S. L. ZACHARIUS
Mechanics and Materials Technology Center
Technology Operations

Prepared for

SPACE AND MISSILE SYSTEMS CENTER
AIR FORCE MATERIEL COMMAND
2430 E. El Segundo Boulevard
Los Angeles Air Force Base, CA 90245

Engineering and Technology Group

APPROVED FOR PUBLIC RELEASE;
DISTRIBUTION UNLIMITED

This report was submitted by The Aerospace Corporation, El Segundo, CA 90245-4691, under Contract No. F04701-88-C-0089 with the Space and Missile Systems Center, 2430 E. El Segundo Blvd., Los Angeles Air Force Base, CA 90245. It was reviewed and approved for The Aerospace Corporation by H. R. Rugge, Acting Principal Director, Mechanics and Materials Technology Center. Capt. Pete Ford was the project officer for the Mission-Oriented Investigation and Experimentation (MOIE) program.

This report has been reviewed by the Public Affairs Office (PAS) and is releasable to the National Technical Information Service (NTIS). At NTIS, it will be available to the general public, including foreign nationals.

This technical report has been reviewed and is approved for publication. Publication of this report does not constitute Air Force approval of the report's findings or conclusions. It is published only for the exchange and stimulation of ideas.

Pete Ford, Captain USAF
Propulsion and Mechanical Branch
Upper Stages Engineering

Wm. Kyle Sneddon, Captain USAF
Deputy, Industrial & International Division

REPORT DOCUMENTATION PAGE

Form Approved
OMB No. 0704-0188

1. AGENCY USE ONLY (*Leave blank*)	2. REPORT DATE	3. REPORT TYPE AND DATES COVERED
	22 August 1993	

4. TITLE AND SUBTITLE
An Ultrasonic Testing Technique for Monitoring the Cure and Mechanical Properties of Polymeric Materials

5. FUNDING NUMBERS
F04701-88-C-0089

6. AUTHOR(S)
Johnson, Eric C.; Pollchik, Jessica D.; Zacharius, Sherrie L.

7. PERFORMING ORGANIZATION NAME(S) AND ADDRESS(ES)
The Aerospace Corporation
Technology Operations
El Segundo, CA 90245-4691

8. PERFORMING ORGANIZATION REPORT NUMBER
TR-93(3935)-12

9. SPONSORING/MONITORING AGENCY NAME(S) AND ADDRESS(ES)
Space and Missile Systems Center
Los Angeles Air Force Base
Los Angeles, CA 90009-2960

10. SPONSORING/MONITORING AGENCY REPORT NUMBER
SMC-TR-93-64

11. SUPPLEMENTARY NOTES

12a. DISTRIBUTION/AVAILABILITY STATEMENT
Approved for public release; distribution unlimited

12b. DISTRIBUTION CODE

13. ABSTRACT (*Maximum 200 words*)

Thin specimens (~10 mils) can be tested using an ultrasonic technique to determine their moduli and Poisson's ratio. For this report, the thin specimen's ultrasonic response is FFT analyzed in an attempt to extend the technique for cure monitoring of polymeric systems. Two such systems are examined and the ultrasonic results compared with differential scanning calorimetry and dynamic mechanical measurements. Two parameters were measured as a function of time: the ultrasonic peak frequency and amplitude. The results suggest that it may be possible to monitor the cure through observation of these two parameters.

14. SUBJECT TERMS
Ultrasonics, Propellant, Solid Rocket Motors, Cure Monitoring, Poisson's Ratio

15. NUMBER OF PAGES
19

16. PRICE CODE

17. SECURITY CLASSIFICATION OF REPORT	18. SECURITY CLASSIFICATION OF THIS PAGE	19. SECURITY CLASSIFICATION OF ABSTRACT	20. LIMITATION OF ABSTRACT
UNCLASSIFIED	UNCLASSIFIED	UNCLASSIFIED	

NSN 7540-01-280-5500

Standard Form 298 (Rev. 2-89)
Prescribed by ANSI Std. Z39-18
298-102

PREFACE

The authors gratefully acknowledge the assistance of R. C. Savedra with sample preparation and data acquisition, R. M. Castaneda with the DSC measurements, and Dr. R. J. Zaldivar with the dynamic mechanical tests.

CONTENTS

FIGURES

INTRODUCTION

Large space booster solid-rocket motors (SRMs) contain composite propellant materials based on either a hydroxyl terminated polybutadiene (HTPB) or the terpolymer of butadiene, acrylic acid, and acrylonitrile (PBAN) polymer matrix. Mechanical tests have revealed significant batch-to-batch variances and age related changes in the propellant moduli[1] probably due to continued crosslinking of the system. This paper documents a work in progress directed toward testing the feasibility of using ultrasonic measurements of the propellant mechanical properties to monitor the condition and the degree of cure of the propellant. If the ultrasonic shear and longitudinal velocities, c_S and c_L, and the density, ρ, of the propellant are known, the Young's modulus, shear modulus, bulk modulus, and Poisson's ratio, E, μ, K, and σ, respectively, can be calculated via the familiar relations,

$$E=\frac{\rho c_L^2(1-2\sigma)(1+\sigma)}{1-\sigma},\ \mu=\rho c_S^2,\ K=\frac{E}{3(1-2\sigma)},\ \text{and}\ \sigma=\frac{c_L^2-2c_S^2}{2c_L^2-2c_S^2} \tag{1}$$

Considerable effort under the NASA Solid Propulsion Integrity Program (SPIP) has been directed along a similar vein.[2] The work presented here is unique in that a simple ultrasonic resonance technique which permits measurement of the acoustic velocities of thin adhesive material specimens is employed. The technique incorporates a slight modification of what was presented in earlier work[3] in that Fast Fourier Transforms (FFTs) are used to process the signals. The technique is characterized by a number of advantages. The same specimen and transducer pair is used to determine both the shear and longitudinal response. In addition, a fluid medium is employed to couple sound into the specimen, thereby eliminating many of the problems associated with the bonding of transducers. Preliminary SPIP results suggest that measurements of the propellant shear velocity are important, but difficult to perform, as the propellant material is very attenuative to shear waves. The hope is that use of thin specimens will serve to mitigate this difficulty.

TECHNIQUE

To understand the technique, consider first a thin medium having acoustic impedance, Z_2, sandwiched between two semi-infinite media of acoustic impedance, Z_1, as depicted in Fig. 1. Assuming a continuous plane-wave stimulation in one of the semi-infinite media, the coefficient of acoustic power transfer, P_T, across the thin medium can be calculated;

$$P_T = \frac{4Z_2^2Z_1^2}{\left(Z_1^2 + Z_2^2\right)^2 \sin^2\left(\frac{2\pi x_2 f}{c}\right) + 4Z_2^2Z_1^2 \cos^2\left(\frac{2\pi x_2 f}{c}\right)} \tag{2}$$

where f is the frequency of the plane wave, c is the acoustic velocity (either shear or longitudinal) and x_2 is the thickness of the thin medium (see Ref. 3).

In Fig. 2, P_T is plotted as a function of frequency for the case where Z_1 = 17 Rayls (aluminum) and Z_2 = 1.48 Rayls (water). It can be seen that the condition of maximum power transmission occurs when $f = f_R = nc/2x_2$, where n is an integer. Note that the thin medium was assumed to be lossless in the derivation of Eq. 2. Taking attenuation into account, one would expect the amplitude of the local maxima to decrease with increasing n.

The experimental apparatus is depicted in Fig. 3. Two aluminum blocks were cut from square rod stock, each having a 74° and 90° face with respect to one side of the block. A milled finish was determined to be adequate on the 74° faces. The 90° faces were lapped to ensure that the surfaces were flat. A thin uniform layer of the specimen being tested was sandwiched between the 90° faces. The spacing between these faces and hence, the specimen thickness, was determined by two identical, stainless-steel wire spacers. To hold this Al/specimen/Al sandwich together, a small rubber O-ring was stretched over a set of threaded pegs located on each of two opposite sides of the sandwich as shown. The depth of thread for these pegs was less than 0.125 inches. The resultant Al/specimen/Al sandwich was set upon a fixture (not included in Fig. 3 for clarity) and submerged in a water tank so as to be centered between a pair of plane wave, through-transmission, ultrasonic transducers. The fixture was designed to permit rotation of the specimen

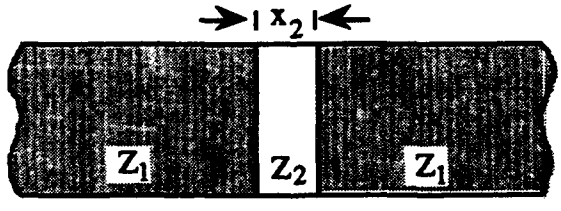

Figure 1. A thin medium of acoustic impedance, Z_2, and thickness, x_2, sandwiched between two semi-infinite media of acoustic impedance, Z_1.

with respect to the transducers. The apparatus was designed to approximate the conditions leading to the derivation of Eq. 2. The Al blocks correspond to the semi-infinite media, the specimen to the thin medium.

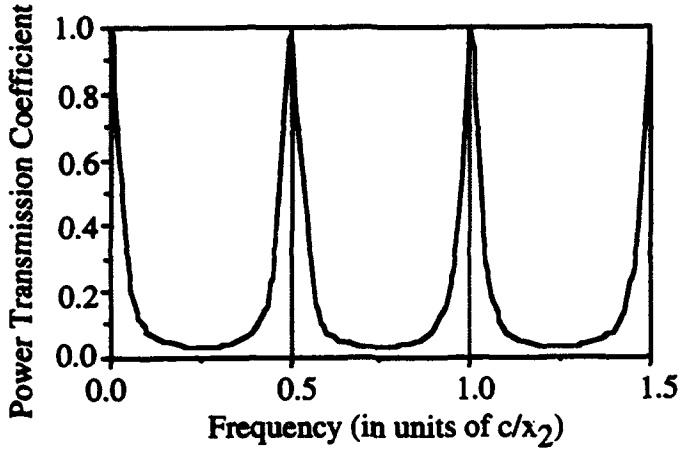

Figure 2. The coefficient of acoustic power transmission across the thin medium as a function of frequency (Eq. 2) for the three layer system depicted in Fig. 1, where Z_1 = 17 Rayls (Al) and Z_2 = 1.48 Rayls (water).

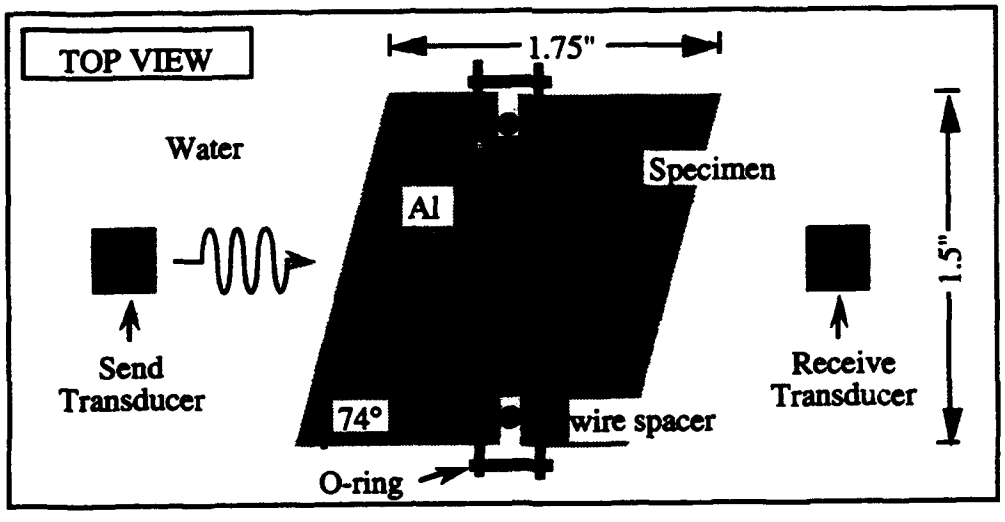

Figure 3. The experimental apparatus as described in the text. As indicated, this is a top view. The Al/specimen/Al sandwich extends 1.5 inches from top to bottom into the page. The transducers and O-ring are bisected by a plane parallel to that of the page and 0.75 inches into the page.

To perform measurements, the send transducer was stimulated with a spike pulse. The fixture was aligned so that this pulse would strike the first 74° face of the Al/specimen/Al sandwich at a particular angle of incidence, θ_i, to its normal, giving rise to both a longitudinal and a shear wave pulse within the aluminum. The longitudinal and shear wave emergence angles for a particular θ_i can be determined using Snell's law.

In the first phase of the experiment, θ_i was set at ~ 3.7° so that the longitudinal pulse transmitted through the first 74° face would strike the Al-specimen interface at normal incidence, and then travel through the remainder of the Al/specimen/Al sandwich to produce a pulse at the receive transducer. This pulse will be referred to as the longitudinal response. Because the longitudinal velocity in Al exceeds that of the shear, the longitudinal response was the first pulse detected after each drive pulse. This first pulse was followed by others due to the shear wave transmitted through the first 74° face and various internal reflections within the sandwich. Upon reception by the receive transducer, the longitudinal response was isolated and its FFT computed. To isolate the effect of the specimen, this FFT was divided by an FFT of the longitudinal response for a reference block comprised of solid Al and having the same dimensions as the Al/specimen/Al sandwich. The corrected data set was then normalized and stored for analysis. A computer was used to automate the system so that the longitudinal response could be measured repeatedly as a function of a specimen's cure time, t. Peaks in the longitudinal response FFT, which in accordance with Eq. 2 occur when $f = f_{RL} = nc_L/2x_2$, could then be used to determine c_L, the longitudinal acoustic velocity of the specimen for each measurement.

In the second phase of the experiment, θ_i was set to ~ 7.5° so that the direction of the transmitted shear wave was normal to the Al-specimen interface. The first received pulse resulting from this normal shear wave will be referred to as the shear response. Following each drive pulse, the shear response was preceded by not only the longitudinal response, but also other signals resulting from internal reflections involving the faster longitudinal pulse. To positively identify the shear response, one could increase θ_i beyond the critical angle for longitudinal wave production in the aluminum so that the shear response would be the first remaining pulse. One could then track this signal while decreasing θ_i to the appropriate value. The FFT of the shear response was then computed, normalized, and stored in the same manner as that of the longitudinal response. Peaks in the shear response FFT, occurring when $f = f_{RS} = nc_S 2x_2$, could then be used to determine the shear acoustic velocity of the specimen, c_S.

RESULTS

Three materials were tested: water; EPON 828, a Shell bisphenol-A/epichlorohydrin-based epoxy system, cured with diethylenetriamine (TETA); and an inert HTPB propellant mixture with sodium chloride substituted for the ammonium perchlorate found in live propellant.

Water was tested first to provide an end-to-end system check, as its acoustic velocity is well known. An Al/H_2O/Al sandwich with wire spacers of diameter $x_2 = 6$ mil was prepared. The longitudinal response for the 6-mil water specimen and its FFT are plotted in Figs. 4a and 4b, respectively. The longitudinal response and its FFT for the reference block under the same conditions are plotted in Figs. 4c and 4d. The FFT for the reference block (Fig. 4d) reflects the fact that 5-MHz transducers were used for the measurement. Comparison of Fig. 4a with Fig. 4c (and Fig. 4b with 4d) reveals that the 6-mil water specimen functioned like a bandpass filter for the input pulse. Dividing the reference block FFT (Fig. 4d) into that of the 6-mil water specimen (Fig. 4b) and normalizing the result yielded the plot depicted in Fig. 5. Note that as expected (compare with Fig. 2), multiple, equally spaced peaks of diminishing amplitude are present. The results for frequencies outside the active range of the transducer, ~ 2 - 7.5 MHz (Fig. 4d),

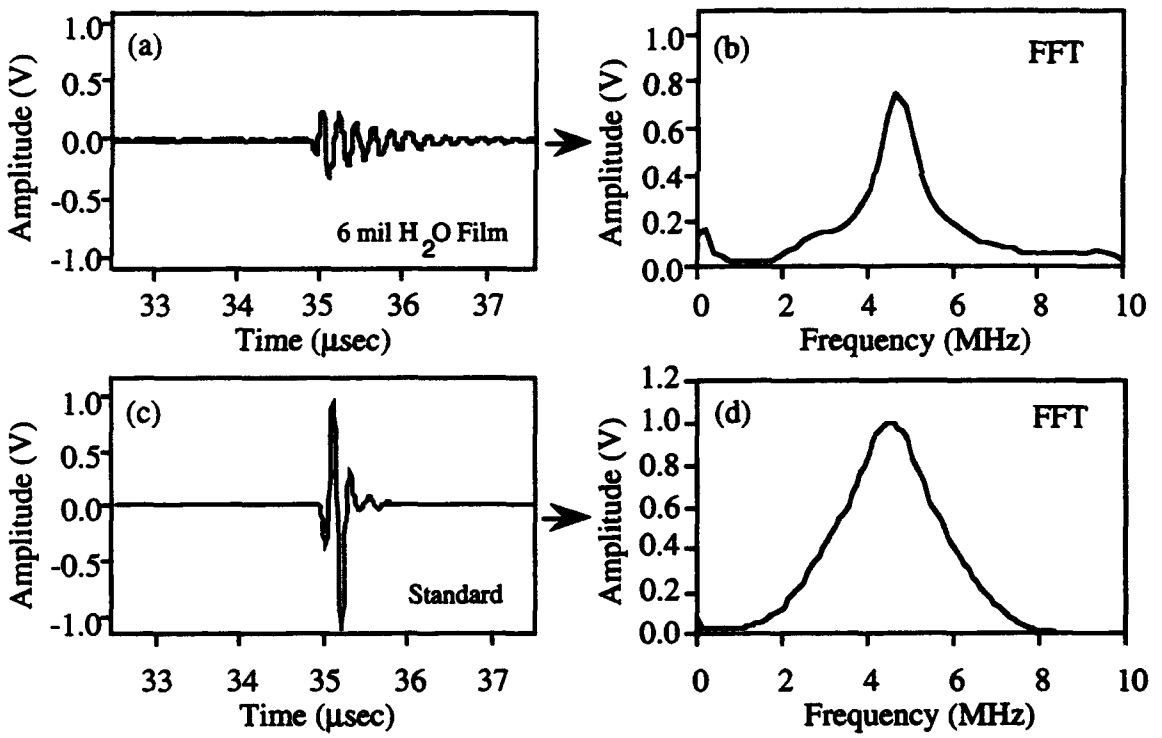

Figure 4. System check: (a) Longitudinal response of the Al/H_2O/Al sandwich. (b) FFT of the Al/H_2O/Al sandwich longitudinal response. (c) Longitudinal response of Al reference block. (d) FFT of the reference block longitudinal response.

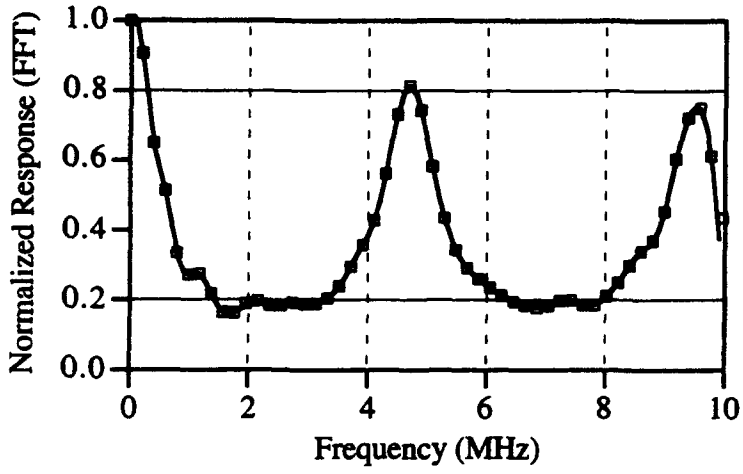

Figure 5. System check: Normalized results from division of the FFTs in Figure 4b and 4d. The first non-zero maxima occurs at 4.69 MHz.

however, should be accepted with caution. From the position of the first non-zero maxima one can calculate $c_L = 2f_{RL}x_2 = 0.056$ in./μs, which compares favorably with the literature value for water of 0.058 in./μs. The slight difference was traced to the fact that the reference block was not cut from the same Al stock as the blocks used for the 6-mil water specimen.

Secondly, tests were performed on the system consisting of a 10:1 mixture of EPON 828 and diethylenetriamine (TETA) hardener. A typical plot of the longitudinal FFT for this system is presented in Fig. 6a. This plot was produced from data acquired following a cure time of $t = 14.5$ min. Three maxima are clearly evident. The third peak is distorted, but it occurs beyond the normal operating range of the 5.0-MHz transducers employed. The thickness of the longitudinal specimen was 10.25 mils. The position of the first maxima implies that $c_L = 0.062$ in./μs. Measurements of the shear response for the EPON 828 system were more difficult. The FFTs obtained varied erratically during the early part of the cure. This is not surprising as liquids do not support shear waves, but at some point a transition must take place. The shear response FFT for $t = 2$ days is plotted in Fig. 6b. A pair of 2.25-MHz transducers were used to accumulate these data. Again, as expected, multiple peaks of diminishing amplitude were observed. The thickness of this specimen was 10.25 mils. The position of the first non-zero maxima implies that $c_S = 0.022$ in/μs. More work involving the shear response will be required before consistent trends can be identified.

The value of c_L for the EPON 828/TETA system changed significantly as the specimen cured, so that the peak positions shifted as depicted in Fig 7a, where plots for $t = 6.3$ min and $t = 96.3$ min are presented. The position of the primary longitudinal peak as a function of cure time is plotted as a solid line in Fig. 7b. It can be observed that the peak position, and hence longitudinal velocity, increased by ~ 45% during the first 6 hours of cure. The amplitude of the longitudinal FFT peaks also changed as a function of cure as indicated by the curve with open boxes in Fig. 7b. The amplitude change is not evident in Fig. 7a, because the data have been normalized. It can be seen that the amplitude decreased during the first 1.5 hours of cure, suggesting that the specimen became more attenuative to sound. The amplitude then rebounded, increasing to

slightly above its original value, before decreasing abruptly to a value which remained essentially constant for the last hour recorded.

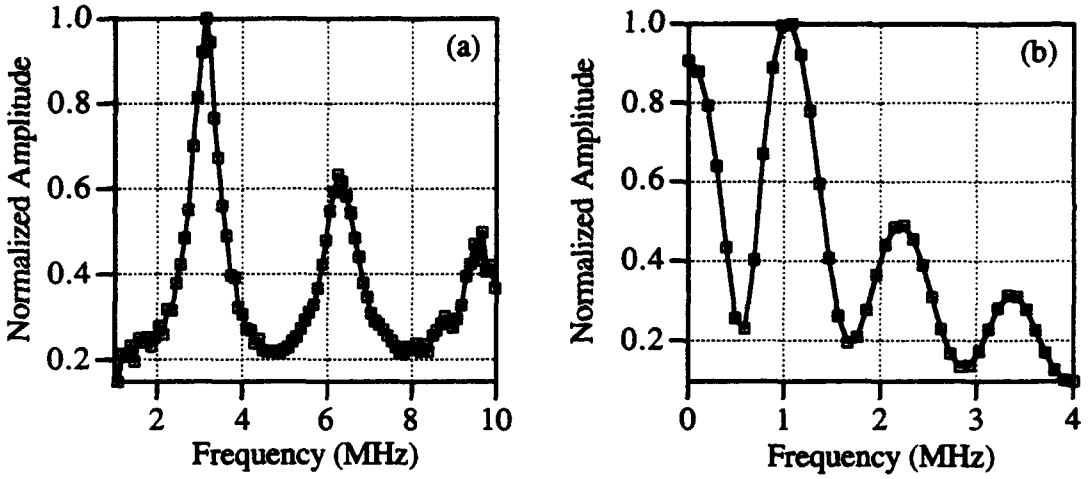

Figure 6. (a) Longitudinal response FFT of EPON 828/TETA mixture at t = 14.5 min. (b) Shear response FFT of EPON 828/TETA mixture at t = 2 days.

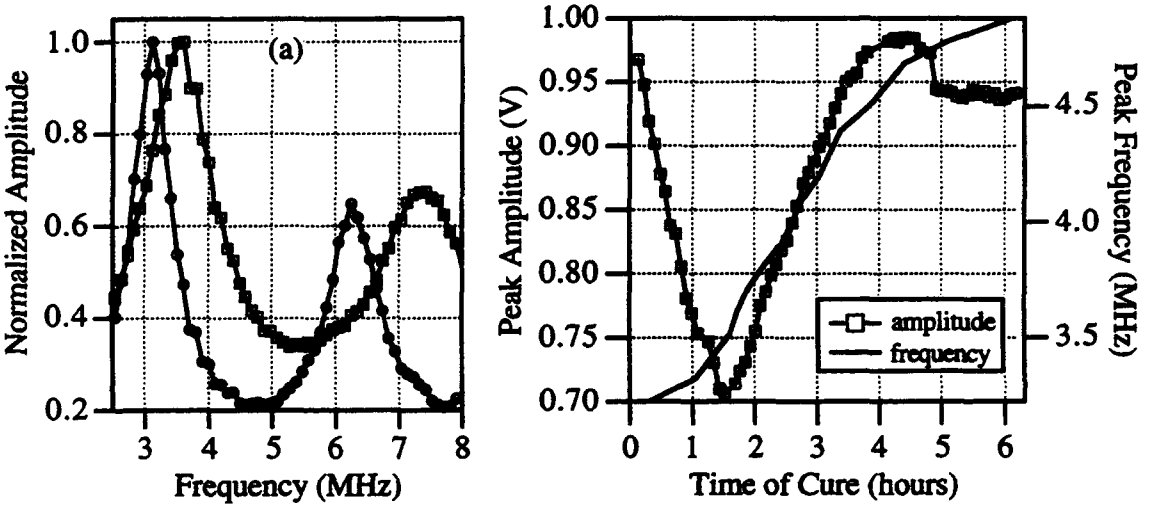

Figure 7. (a) Longitudinal response FFT at t = 6.3 min (circles) and t = 96.3 min (squares) and (b) the change in amplitude and resonant frequency as a function of t for an EPON 828/TETA specimen.

For comparative purposes, differential scanning calorimetry (DSC) was performed on a number of EPON 828 samples. By measuring the heat of reaction (ΔH) as a function of time beginning with the mix, one can estimate the degree of cure. The ΔH measured for a sample at $t = 0$ corresponds to 0% cure, and when $\Delta H = 0$ the system is considered 100% cured. Thus a plot of ΔH versus time provides a correlation between the degree of cure and time, which can then be applied to the peak amplitude and frequency versus time data (Fig. 7b). The ΔH measurements were performed on a Mettler DSC 30 with a Mettler TC 10A TA processor. The DSC results for a sample taken from the same mix as that which led to Fig. 7 are plotted in Fig. 8. Each data point in Fig. 8 was measured on a separate sample and represents the residual heat of reaction remaining in the sample at time x. For the EPON 828/TETA system there is a significant amount of heat generated as the two oxirane groups of the EPON 828 react with the amine group of the TETA (an aliphatic polyamine) to produce a three-dimensional, crosslinked network. This reaction occurs at room temperature (RT) and requires several days (at RT) or one to two hours at 100 °C to reach complete cure.

In addition to DSC, a Rheometrics RDA II was employed to measure the epoxy system's viscosity, elastic modulus (G'), viscous modulus (G''), and damping or loss tangent ($\tan \delta = G''/G'$) as a function of time from initial mixing. The RDA measures these viscoelastic parameters in dynamic shear using a parallel-plate fixture. The measurements were made at a constant temperature of 27° C. The RDA II results, which are presented in Fig. 9, give insight into the behavior exhibited by the peak amplitude curve of Fig. 7b. As expected, the viscosity increases with time. This is due to the constant increase in molecular weight of the epoxy as crosslinking occurs. Similarly, G' and G'' (the real and imaginary parts of the dynamic shear modulus) increase with time. The G' begins its ascent at approximately the same time that the peak-amplitude curve of Fig. 7b exhibits a minimum. The slight difference in time is probably related to the fact that the ultrasonic measurements were performed at RT as opposed to 27° C. This same phenomenon is reflected as a maximum in the tan δ curve and is most likely associated with the onset of crosslinking for the epoxy. The gel point is traditionally defined as the point at which G' and G'' cross.[4] The dynamic mechanical testing was terminated at ~ 2.2 hours as the viscosity of the sample exceeded the torque limits of the instrument.

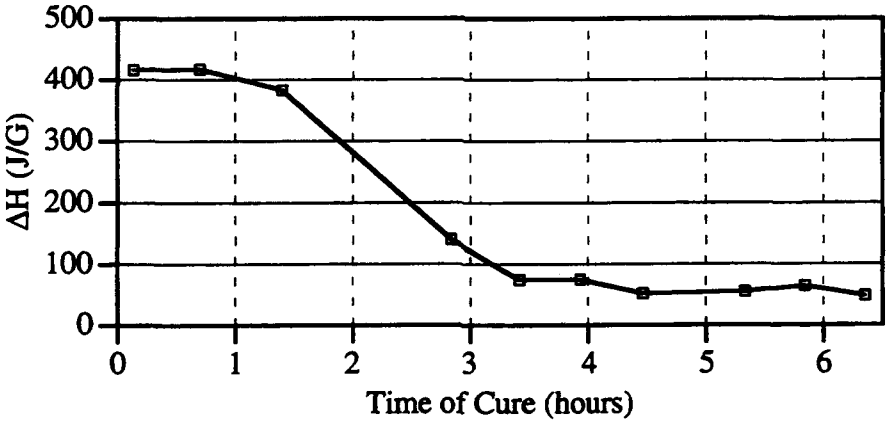

Figure 8. Heat of reaction (ΔH) versus time of cure for the same EPON 828/TETA mixture as that used for the data of Fig. 7.

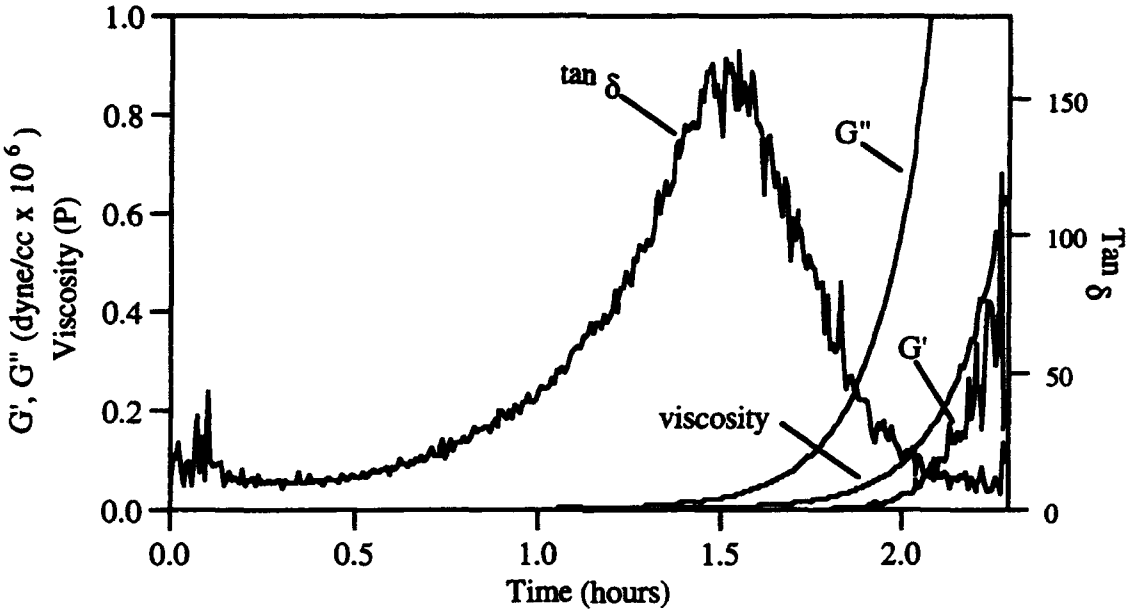

Figure 9. Viscosity, G', G'', and tan δ vs time for the EPON 828/TETA mixture.

Finally, measurements were performed on HTPB inert-propellant specimens. The first difficulty encountered was that it was difficult to compress the material to form samples thinner than 10 mils. The longitudinal response FFT for a 10-mil specimen is plotted in Fig. 10a. Two peaks are clearly visible; the second riding on the tail of the first. The position of the primary peak implies that $c_L = 0.043$ in./μs, a value ~ 20% slower than that of water. This value remained essentially constant as a function of cure, perhaps a reflection of the high solid content of the inert propellant. The amplitude of the primary peak did, however, vary significantly with cure time, as indicated by the plot depicted in Fig. 10b. The form of the plot is similar to that of the EPON 828/TETA mixture in that the amplitude decreases during the beginning stages of the cure and then rebounds to nearly its initial value. The results differ in that following the rebound, the signal drops monotonically, except for a curious upswing at t_c ~ 30 hours, to a lower value than that achieved in the early stages of the cure. Preliminary attempts to perform a DSC of the inert propellant were unsuccessful. This is attributed to the high filler content. For the purposes of thermal analysis, the filler, which has a high specific heat, absorbs energy and reduces the exotherm temperature. Additionally, because the DSC sample size is small, on the order of 20 mg, the filler has the effect of reducing the amount of material involved in the curing reaction, and thus reducing the exotherm. Measurements of the shear response of the inert propellant were less successful than those for the EPON 828/TETA mixture. Again, more work involving the shear response will be required before consistent trends can be identified.

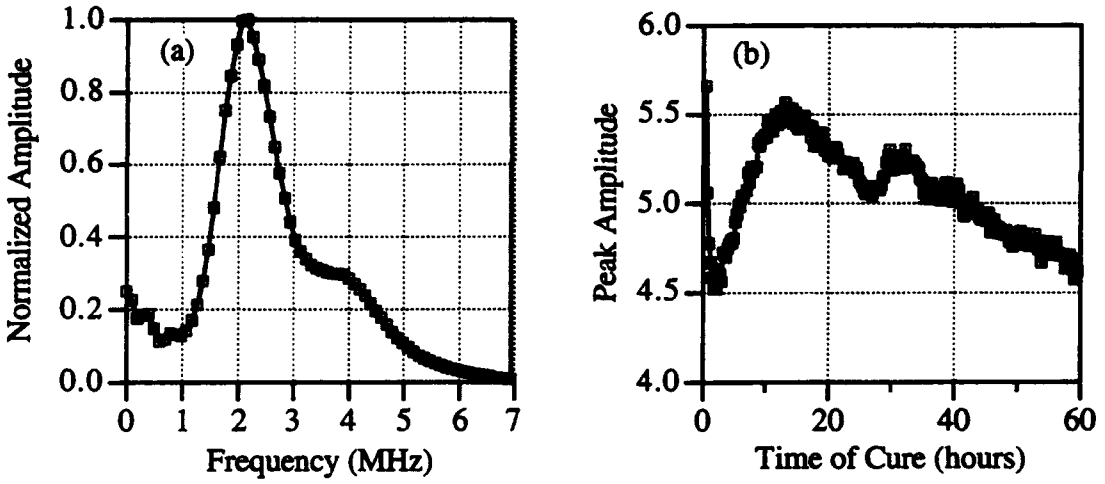

Figure 10. (a) Longitudinal response FFT and (b) the change in amplitude as a function of cure time for a HTPB inert propellant specimen.

DISCUSSION

The ultrasonic resonance technique described in this work exhibits potential as a means of monitoring the degree of cure as well as cure- and age-related mechanical property changes in polymers. Preliminary results indicate that the changes in the peak frequency (ultrasonic velocity) data can be correlated with the degree of cure and that the changes in the peak amplitude can be related to the results of dynamic mechanical tests. The results presented in this report suggest that SRM propellants are particularly difficult materials to characterize, especially in the frequency range employed in these tests. Much of the difficulty probably stems from the high solid content of the propellant. It may be prudent to perform similar tests on unfilled HTPB specimens. In addition, future tests (particularly for the shear mode) should be performed at lower frequencies and, perhaps, different temperatures.

REFERENCES

1. P. H. Graham, "Analysis of the Variability of HTPB Propellant Mechanical Properties," *Annual report for NASA Marshall Space Flight Center under Contract No. NAS8-37802*, Report No. 443/1290/36, 12 Dec. 1990.

2. M. Rooney, C. L. Friant, C. V. O'Keefe, and W. M. Ferrell, "Determination of Modulus of HTPB Solid Rocket Propellant using Longitudinal and Shear Ultrasonic Waves," *Annual report for NASA Marshall Space Flight Center under Contract No. NAS8-37802*, Report No. 443/1291/37, pp. 43-55.

3. E. C. Johnson, J. D. Pollchik and J. N. Schurr, "An Ultrasonic Testing Technique for Measurement of the Poisson's Ration in Tin adhesive Layers," *Review of Progress in Quantitative Nondestructive Evaluation* (edited by D. O. Thompson and D. E. Chimenti, Plenum Press, New York, 1992), Vol 11B, 1291-1298 (1992).

4. C. M. Long, and P. J. Dynes, "Relationships Between Viscoelastic Properties and Gelation in Thermosetting Systems," *J. App. Poly. Sci.*, Vol 27, 569-574 (1982).

TECHNOLOGY OPERATIONS

The Aerospace Corporation functions as an "architect-engineer" for national security programs, specializing in advanced military space systems. The Corporation's Technology Operations supports the effective and timely development and operation of national security systems through scientific research and the application of advanced technology. Vital to the success of the Corporation is the technical staff's wide-ranging expertise and its ability to stay abreast of new technological developments and program support issues associated with rapidly evolving space systems. Contributing capabilities are provided by these individual Technology Centers:

Electronics Technology Center: Microelectronics, solid-state device physics, VLSI reliability, compound semiconductors, radiation hardening, data storage technologies, infrared detector devices and testing; electro-optics, quantum electronics, solid-state lasers, optical propagation and communications; cw and pulsed chemical laser development, optical resonators, beam control, atmospheric propagation, and laser effects and countermeasures; atomic frequency standards, applied laser spectroscopy, laser chemistry, laser optoelectronics, phase conjugation and coherent imaging, solar cell physics, battery electrochemistry, battery testing and evaluation.

Mechanics and Materials Technology Center: Evaluation and characterization of new materials: metals, alloys, ceramics, polymers and their composites, and new forms of carbon; development and analysis of thin films and deposition techniques; nondestructive evaluation, component failure analysis and reliability; fracture mechanics and stress corrosion; development and evaluation of hardened components; analysis and evaluation of materials at cryogenic and elevated temperatures; launch vehicle and reentry fluid mechanics, heat transfer and flight dynamics; chemical and electric propulsion; spacecraft structural mechanics, spacecraft survivability and vulnerability assessment; contamination, thermal and structural control; high temperature thermomechanics, gas kinetics and radiation; lubrication and surface phenomena.

Space and Environment Technology Center: Magnetospheric, auroral and cosmic ray physics, wave-particle interactions, magnetospheric plasma waves; atmospheric and ionospheric physics, density and composition of the upper atmosphere, remote sensing using atmospheric radiation; solar physics, infrared astronomy, infrared signature analysis; effects of solar activity, magnetic storms and nuclear explosions on the earth's atmosphere, ionosphere and magnetosphere; effects of electromagnetic and particulate radiations on space systems; space instrumentation; propellant chemistry, chemical dynamics, environmental chemistry, trace detection; atmospheric chemical reactions, atmospheric optics, light scattering, state-specific chemical reactions and radiative signatures of missile plumes, and sensor out-of-field-of-view rejection.